Current Biology, Volume *30*

Supplemental Information

FGF Pyramus Has a Transmembrane Domain and Cell-Autonomous Function in Polarity

Vincent Stepanik, Jingjing Sun, and Angelike Stathopoulos

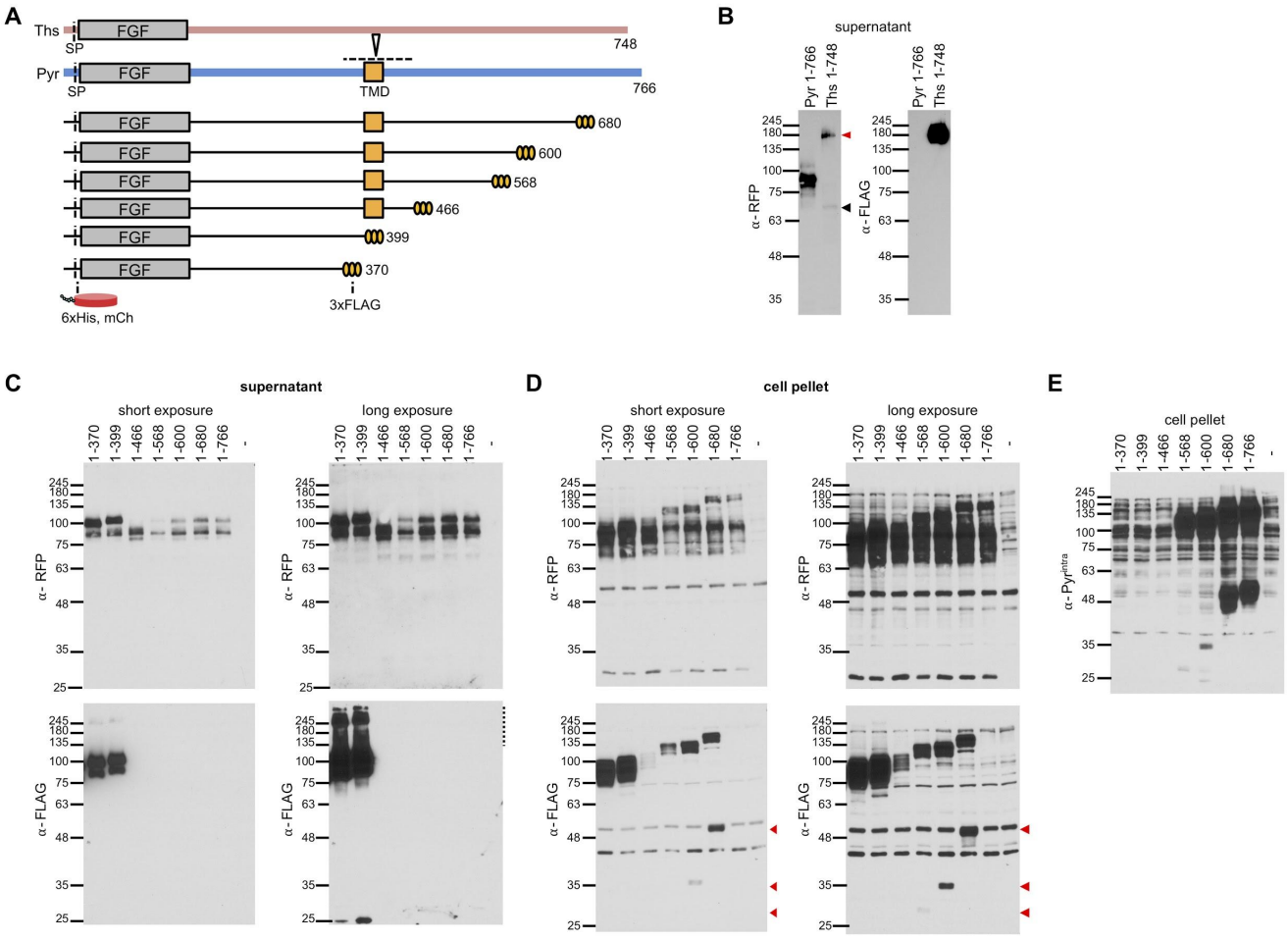

Figure S1. Longer exposures and extended molecular weight ranges of western blots. Related to Figures 1 and 3.

(A) Schematic showing the domain structure of Ths and Pyr, including the signal peptide (SP), FGF domain, and transmembrane domain (TMD) of Pyr. Truncations expressed in S2 cells for Figure 1D-G and D-F below are shown, with a 6xHis,mCh tag inserted before the FGF domain of each, and a 3xFLAG tag at the C-terminus, including the full-length Ths and Pyr shown in B.

(B) Western blots of pulldowns from supernatants of S2 cell transfections of dual-tagged, full-length Ths and Pyr. Black arrowhead is cleaved, N-terminal fragment-only Ths, and red arrowhead is full-length Ths.

(C-E) Western blots of pulldowns from supernatants and total cell extracts of S2 transfected with Pyr truncations. Short and long exposures for each western are shown. Arrowheads indicate isoforms

common to longer truncations and are presumably mature products. Pyr truncations ending at T440 and beyond, tagged at their N-termini with mCh and at their C-termini with 3xFLAG, show FLAG signals that are only detectable intracellularly. In contrast, truncations ending at A370 and T399 show FLAG signals in both the supernatant and intracellularly (Figure S1C,D). Also, for truncations extending beyond T399, the strong correspondence of mCh and FLAG signals is lost, suggesting that at least one proteolytic cleavage site exists in the interval of aa 370-466. (D) Red arrowheads indicate MW of bands with corresponding RFP and FLAG signals of longer truncations that are only present intracellularly. Black arrowhead indicates N-terminal product cleaved from C-terminal sequence, common to truncations C-terminal to aa 370. Dotted line indicates products with range of MW likely due to differential post-translational modifications, and black arrows on longer exposure are shorter Pyr^{intra} forms resulting from the truncations. For the cell pellet samples of Pyr 1-600 and 1-680, red arrowheads indicate FLAG-reactive, non-RFP reactive bands indicative of free, intracellular Pyr C-terminal fragments. For the 1-466 cell pellet sample in Fig 1D, although a weaker FLAG signal is seen relative to the other truncations tested, there is a readily detectable FLAG signal with this longer exposure. We have noticed some variability of FLAG signal detection in western blots depending on amino acid context, which is indicated for 1-466 with the equal strength of RFP signal compared to the other truncations. For the anti-FLAG blot of supernatants in C, the dotted line indicates lower-abundance, higher molecular weight isoforms of the truncations that are FLAG-reactive. The absence of corresponding RFP-reactive signal is likely due to weaker antibody RFP performance.

(E) Longer exposure and extended molecular weight ranges of the western blot in Figure 3B.

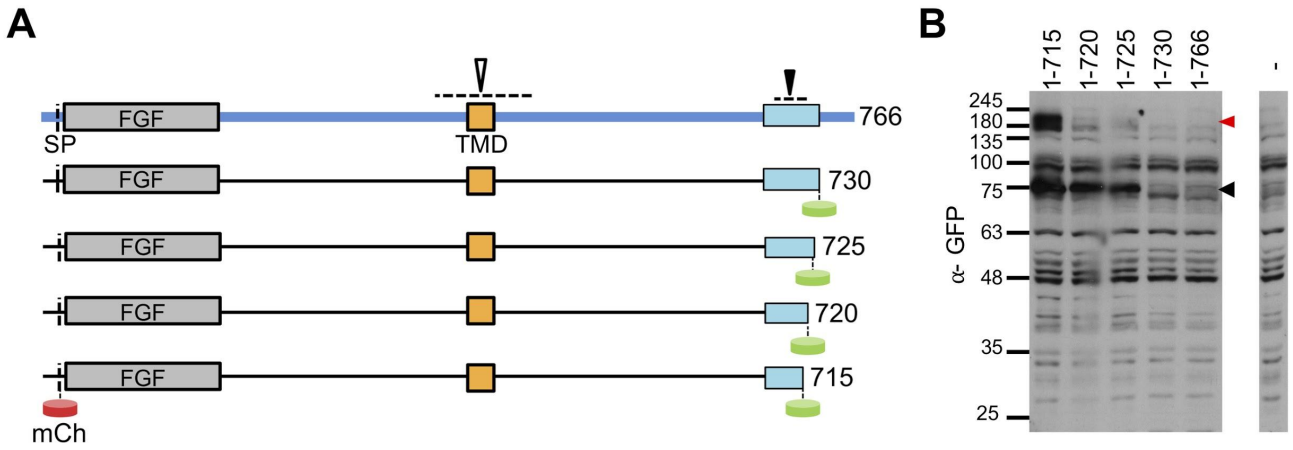

FIGURE S2. The C-terminus of Pyr is undetectable when tagged after amino acid 730. Related to Figure 2.

(A) Schematic of Pyr truncations near the Pyr degron, with a C-terminal GFP tag. SP=signal peptide, TMD= transmembrane domain, red box = degron. Triangles and dashed lines denote approximate location of proteolytic cleavage sites.

(B) Western blot probed with GFP of cell pellet extracts of S2 cells transfected with the indicated truncations, full length (1-766) or non-transfected (-). All lanes were present on the same blot. Panel has been cropped between 1-766 and (-) samples to exclude non-relevant lanes. Red arrowhead indicates intact "full length" mCh-Pyr-GFP truncations, and the black arrowhead indicates Pyr^{intra}-GFP separated from the rest of the Pyr molecule.

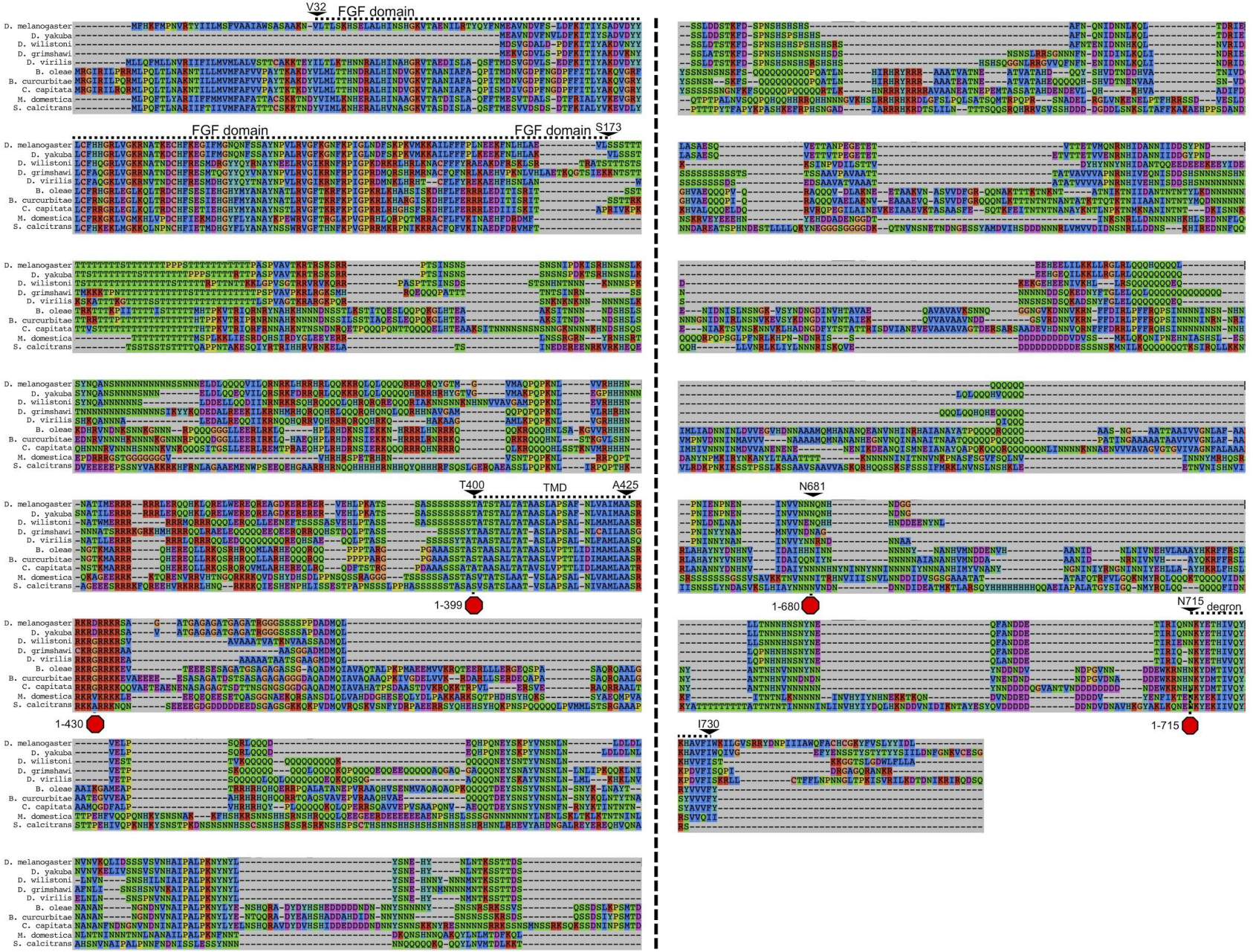
V32
FGF domain
FGF domain
FGF domain
S173
T400
TMD
A425
N681
1-399
1-680
N715
degron
1-430
I730
1-715
D. melanogaster
D. yakuba
D. willistoni
D. grimshawi
D. virilis
B. oleae
B. curcurbitae
C. capitata
M. domestica
S. calcitrans

Figure S3. Multi-sequence alignment of Pyr orthologs in Drosophila and Dipteran flies in the Tephritidae and Muscidae family members. Related to Figures 1 and 2.

MUltiple Sequence Comparison by Log-Expectation (MUSCLE) alignment of Pyr orthologs across representative species of the Drosophilidae, Tephritidae, and Muscidae families of Dipterans. Regions of high conservation of interest are noted including the FGF domain, transmembrane domain and post-TMD stretch of basic residues, degron as well as positions of truncation mutants created using CRISPR/Cas9 (stop sign symbols). Amino acid color code consists of blue=hydrophobic, red=basic, purple=acidic, polar=green, yellow=proline, pink=cysteine, cyan=histidine and tyrosine, orange=glycine.

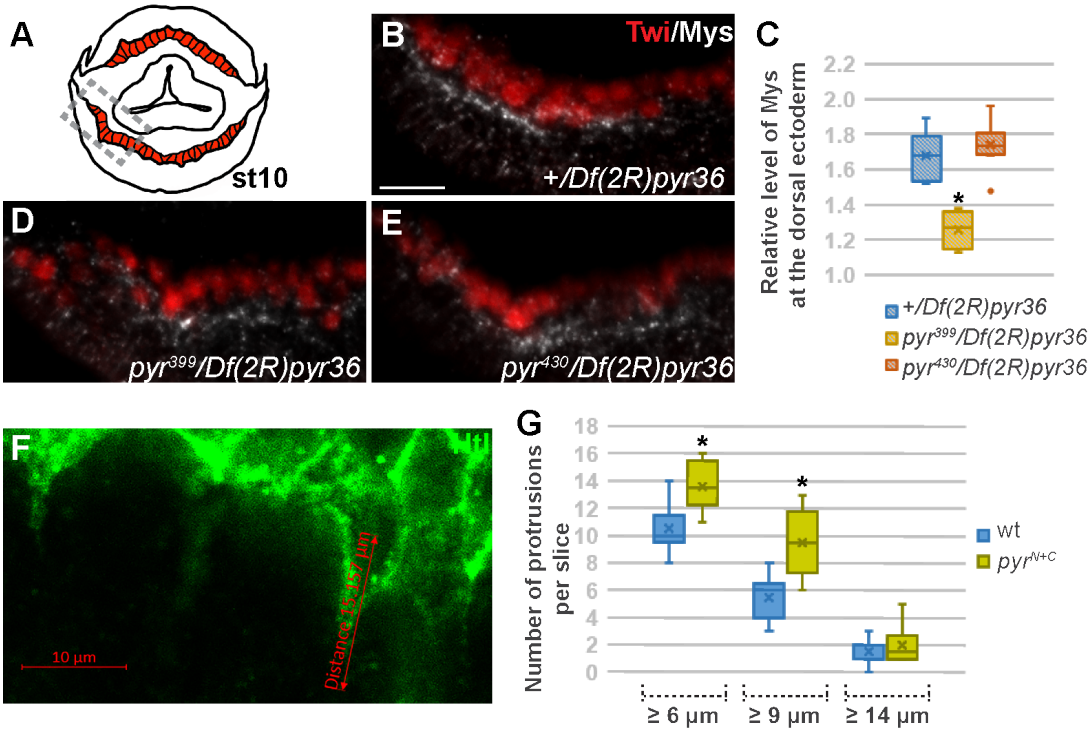

Figure S4. Pyr TMD when connected with the N-terminus supports Mys localization which possibly limits the protrusive activity of mesoderm cells. Related to Figure 5.

(AB,D,E) To assay a role of TMD for localized Mys expression at the dorsal ectoderm-mesoderm interface, either wild-type or truncated *pyr*^{399} and *pyr*^{430} alleles were also crossed into *Df(2R)pyr36* mutant background to eliminate the possible effect of a second-site mutation in homozygous backgrounds (See Methods). Mesoderm cells are marked by anti-Twi immunofluorescence (red), and Mys levels assayed by anti-Mys immunofluorescence signal (white).

(C) Relative difference in Mys expression within the dorsal ectoderm (see boxed region in A) for transheterozygous combinations between CRISPR/Cas9 mutants and a *pyr* null (i.e. *Df(2R)pyr36*) is plotted. The Mys level at the dorsal ectoderm-mesoderm interface in *pyr*^{399}*/Df(2R)pyr36* (D) is significantly lower compared to those in *+/Df(2R)pyr36* (B) or *pyr*^{430}*/Df(2R)pyr36* (E). $n \geq 8$, $p < 0.01$. Genotypes and antibody combination are as indicated. Scale bar, 20 µm.

(F,G) Example of protrusion measurement in Zen software (F). More mesoderm protrusions in *pyr*$^{N+C}$ mutants compared to wild-type embryos suggests that disconnecting of TMD from the N-terminal FGF domain and/or higher levels of Pyr^{intra} promotes the protrusive activity of mesoderm cells ($n \geq 8$, $p < 0.005$) (G).

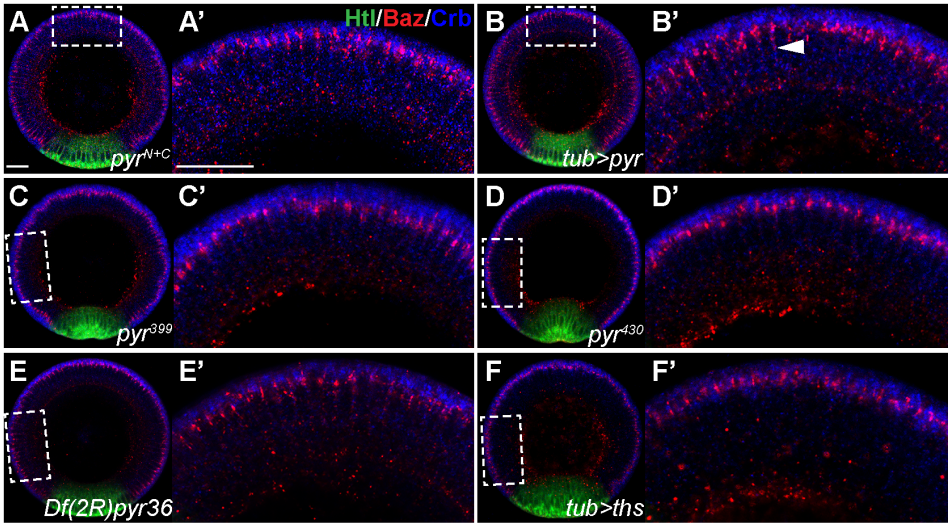

Figure S5. Pyr^{intra} functions cell-autonomously to regulate apicobasal polarity. Related to Figure 7.

(A-F') Expression of Crb (blue) and Baz in stage 6 embryos with magnified views of boxed areas to the right. Baz localization in the dorsal ectoderm extends basally upon ubiquitous overexpression of *pyr* (A'), while it is not affected in the same region in *pyr*$^{N+C}$ mutant embryo (B'). It is also not affected in the neuroectoderm in loss of function *pyr* mutants (C',D',E',F'). Htl antibody (green) is used to mark the mesoderm. Genotypes and antibody combinations are as indicated. Scale bar, 20 µm.

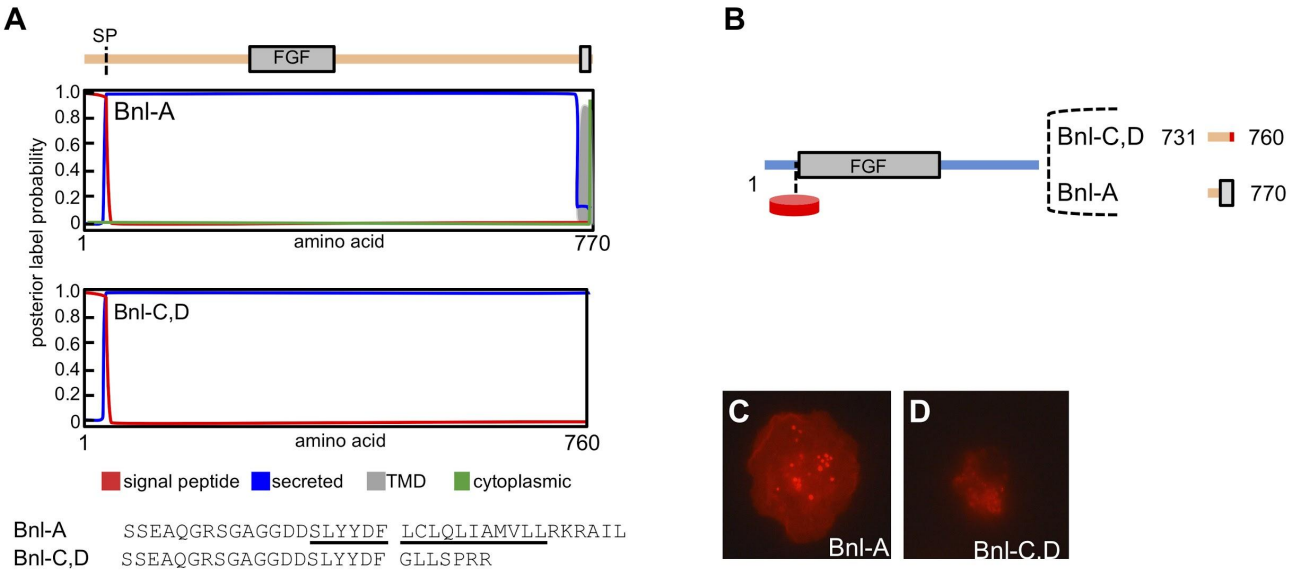

Figure S6. Bnl has a spliceform-specific TMD. Related to Figure 7.

(A) A TMD is predicted at the C-terminus of the Bnl-A spliceform using Phobius, that is not present in Bnl-C and Bnl-D spliceforms. The sequence of the varying amino acids present at the C-terminus are shown at the bottom of the panel.

(B) Schematic of the C-termini of Bnl-A and Bnl-C fused to the C-terminus of mCh-Pyr aa 1-292

(C,D) Expression of the fusions in (B) in S2 cells, with Bnl-A showing localization in both vesicles and at the plasma membrane.